

Intermixing studies in GaN_{1-x}Sb_x highly mismatched alloys

WENDY L. SARNEY^{1*}, STEFAN P. SVENSSON¹, MIN TING^{2,7}, NATALIE SEGERCRANTZ^{2,3}, WLADEK WALUKIEWICZ², KIN MAN YU^{2,4}, ROBERT W. MARTIN⁵, SERGEI V. NOVIKOV⁶, AND C.T. FOXON⁶

¹US Army Research Laboratory, RDRL-SEE-I, 2800 Powder Mill Road, Adelphi, MD, 20783 USA

²Materials Sciences Division, Lawrence Berkeley National Laboratory, 1 Cyclotron Road, Berkeley, CA 94720, USA

³Department of Applied Physics, Aalto University School of Science, PO Box 15100, FI-00076 AALTO, Finland

⁴Department of Physics and Materials Science, City University of Hong Kong, Kowloon, Hong Kong

⁵Department of Physics, SUPA, University of Strathclyde, Glasgow, G4 0NG, UK

⁶School of Physics and Astronomy, University of Nottingham, Nottingham NG7 2RD, UK

⁷Department of Mechanical Engineering, University of California, Berkeley, CA 94720, USA

*Corresponding author: wendy.l.sarney.civ@mail.mil

Received XX Month XXXX; revised XX Month, XXXX; accepted XX Month XXXX; posted XX Month XXXX (Doc. ID XXXXX); published XX Month XXXX

GaN_{1-x}Sb_x with x~ 5-7% is a highly mismatched alloy predicted to have favorable properties for application as an electrode in a photo-electrochemical cell for solar water splitting. In this study, we grew GaN_{1-x}Sb_x under conditions intended to induce phase segregation. Prior experiments with the similar alloy GaN_{1-x}As_x, the tendency of Sb to surfact, and the low growth temperatures needed to incorporate Sb, all suggested that GaN_{1-x}Sb_x alloys would likely exhibit phase segregation. We found that, except for very high Sb compositions, this was not the case, and that instead interdiffusion dominated. Characteristics measured by optical absorption were similar to intentionally grown bulk alloys for the same composition. Furthermore, the alloys produced by this method maintained crystallinity for very high Sb compositions, and allowed higher overall Sb compositions. This method may allow higher temperature growth while still achieving needed Sb compositions for solar water splitting applications.

OCIS codes: (160.6000) Semiconductor materials; (250.0250) Optoelectronics; (310.0310) thin films;

<http://dx.doi.org/10.1364/AO.99.099999>

1. INTRODUCTION

The highly mismatched alloys (HMAs) consist of elements that have large differences in size and electronegativity, resulting in dramatic band structure changes even for dilute substitutions of one of the components of the host alloy. GaN is a robust wide bandgap semiconductor that is traditionally exploited for high power, high temperature applications [1-2]. At the Army Research Laboratory, group III-N alloys such as AlGaIn, are the subject of much past and current research for the application of ultra-violet (UV) emitters [3-5]. We have grown other III-V ternaries and quaternaries where we substituted one of the host alloy's group V element with dilute concentrations of N, such as GaSbN, GaAsN, InAsSbN and InAsN to explore their utility as long wavelength direct bandgap infrared detector materials [6-8]. More recently, and less conventionally, we have also investigated 'dilute As' [9] or 'dilute Sb' alloys of GaN_{1-x}As_x and GaN_{1-x}Sb_x, the latter of which is the subject of this paper.

GaN_{1-x}Sb_x is a promising semiconductor-based HMA for use as a photoelectrode in photoelectrochemical cells (PEC) for solar water splitting due to its expected chemical inertness and favorable band gap as well as band edge positions [10]. Adding small amounts of Sb to GaN drastically reduces the bandgap in accordance with the band anticrossing model (BAC) [11]. The bandgap reduction originates mostly from an upward shift of the valence band edge. This allows for an optimization of the width of the bandgap and the locations of the conduction and valence band edges relative to the water redox

potentials. Thus, ref [12] suggested that the addition of ~5-7% Sb to GaN allows the targeted ~2 eV bandgap, with the conduction and valence bands still straddling the redox potentials. Successful synthesis of such materials with these properties, desired for PEC applications, would allow clean, low-cost production of hydrogen for 'fuel on demand'.

To realize the potential of the GaN_{1-x}Sb_x alloy, a thorough understanding of the dependence of the material properties on the wide range of possible synthesis conditions is necessary. The literature reports few known specifics about which, if any, conditions lead to the synthesis of a practical semiconductor material based on this alloy. The payoff, however, if successful would be enormous, since photolysis is the well-known 'holy grail' of electrochemistry. A material that finally enabled solar water splitting would create a viable alternative to petroleum as an energy source.

Studies of GaN_{1-x}As_x HMAs confirmed that the difference in the electronegativity and the physical size of the N and As atoms made it difficult to obtain high concentrations of As in the alloy before the onset of phase separation. In 2002, Novikov *et al.*, [13] grew GaN_{1-x}As_x with 0.2% As at 800 C with solid source molecular beam epitaxy (MBE). Prior to that work, the maximum concentrations reported by gas-source MBE were x~0.26% [14,15] at a growth temperature of 750°C and x~1% [16] at 500°C, respectively. These results suggest that the solubility limit of As in GaN is a function of temperature [17]. Zhao, *et al.*, [16], has suggested that As acts mainly as a surfactant for temperatures over 700 C and that the GaN surface morphology improved in the presence of As at these high temperatures. In 2009, Yu, *et al.*, [18] reported the growth

of $\text{GaN}_{1-x}\text{As}_x$ across the composition range at extremely low temperatures (~ 200 C). The alloys were amorphous for As compositions ranging between 17% and 75% and were otherwise crystalline.

This showed that since concentrations of $\sim 10\%$ As are needed to produce an alloy with band gap of ~ 2 eV for PEC applications, $\text{GaN}_{1-x}\text{As}_x$ would have to be grown at unconventionally low temperatures, well below the typical GaN growth temperatures of up to 1000 C.

There is not a lot of information about what conditions would allow Sb to incorporate into GaN. Sb has surfactant properties for epitaxial growth under a wide range of growth conditions. Both Sb and As have been used as surfactants to stabilize the growth front during SiGe growth [19-20]. Zhang, *et al.*, used Sb as a surfactant in MOVPE growth of GaN at temperatures of 1000-1100 C and found a slight improvement in the optical and structural properties, particularly for films grown under high V/III ratio conditions [17]. One expects the solid solubility of Sb in GaN to be low due to the large difference in covalent radii and electronegativity, even larger than those for As in GaN [21-22]. Due to this, and because of the known tendency of Sb to surfact, it seemed reasonable to expect growth of $\text{GaN}_{1-x}\text{Sb}_x$ to be even more challenging than $\text{GaN}_{1-x}\text{As}_x$.

In prior reports, we synthesized $\text{GaN}_{1-x}\text{Sb}_x$ over a wide composition spectrum at 80 C [21-23]. At the somewhat higher temperature of 325 C, we grew $\text{GaN}_{1-x}\text{Sb}_x$ with Sb compositions of up to 18% by varying the Sb flux [9]. Although optical absorption measurements indicate that we can produce the ~ 2 eV bandgap with this polycrystalline/amorphous material, for device applications it is necessary to improve the crystalline quality of the material. One of the most obvious ways to achieve this is by raising the growth temperature in the direction of typical GaN growth temperatures, while still maintaining sufficient Sb incorporation. Our prior experiments have shown that, like As in $\text{GaN}_{1-x}\text{As}_x$, the Sb incorporation into $\text{GaN}_{1-x}\text{Sb}_x$ decreases with increasing growth temperature [9]. The challenge is to find growth conditions that allow the incorporation of $\sim 5\text{-}7\%$ Sb at the highest possible growth temperature without inducing phase segregation.

Our growth experiments at 325 C showed no evidence of Sb segregation for Sb concentrations ranging from 2-18%. However, surprisingly we also saw no evidence of the main x-ray diffraction (XRD) film peak from $\text{GaN}_{1-x}\text{Sb}_x$ shifting with Sb incorporation. We saw a single peak corresponding to that expected for (0002) GaN, which decreased in intensity with increasing Sb. This is despite Rutherford backscattering spectroscopy (RBS) and wavelength dispersive spectroscopy (WDS) measurements indicating Sb incorporation, and a corresponding change in the optical absorption edge with increasing Sb composition. We also did not observe separate GaSb features in the XRD diffraction that would have indicated phase separation as has been seen previously in $\text{GaN}_{1-x}\text{As}_x$ [18]. Prior reports noted anomalous XRD results in the dilute-nitride $\text{GaSb}_{1-x}\text{N}_x$ system, although the dilute-nitride $\text{GaN}_{1-x}\text{As}_x$ system XRD results showed no discrepancy related to SIMS results [24-25]. On both the dilute Sb and dilute N extremes, it appears that the interaction of N with Sb is fundamentally different than the interaction of N with As. These perplexing observations still require explanation.

To better understand the tendencies for Sb to segregate or interdiffuse in the $\text{GaN}_{1-x}\text{Sb}_x$ alloy system we designed an experiment in which a series of samples were grown by alternately cycling the Sb and N shutters in a plasma assisted MBE system, which should in effect create a GaN/GaSb multilayer, in particular if phase separation is strong. We could use such a structure as a digital alloy, superlattice, or multilayer structure depending on the duty cycle of the repeated cells. Furthermore, a structure consisting of two binary layers might be easier to grow (control) than a bulk layer consisting of $\text{GaN}_{1-x}\text{Sb}_x$. It may also

be easier, and advantageous, to grow these structures at higher growth temperatures, without losing Sb as exhibited in the bulk alloys.

2. EXPERIMENT

We grew the structures in a GENII MBE system with a Veeco Uni-bulb plasma source to provide active N, elemental Ga and a Veeco valved cracker-source for Sb. For all samples, we set the uncoated, 2-inch epitaxially sapphire substrate temperature by thermocouple to 325 C. The Ga cell was set to a temperature corresponding to a GaN growth rate on sapphire of $0.278 \text{ \AA}/\text{sec}$ or $0.100 \text{ \mu m}/\text{hr}$ and a GaSb growth rate on GaSb of $0.25 \text{ \mu m}/\text{hr}$.

We examined the structural morphology with cross sectional transmission electron microscopy (TEM) and high resolution XRD, and assessed chemical compositions with RBS and WDS. The bandgaps were determined by optical absorption in the spectral range of 250-2500 nm measured using a Perkin Elmer Lambda 950 Spectrophotometer.

One 0.36 \mu m baseline GaN structure with no Sb was grown. The remaining 7 samples had a 25.6 nm GaN buffer layer followed by the intended GaN/GaSb multilayer region, followed by a 12.8 nm GaN cap layer. We will refer to the intended multilayer region as the active region in the following. The thickness of the active region ranged from 0.21 to 0.31 \mu m . The structures have various repeating cell thicknesses, as shown in Fig 1a, with the relative percentage of the structure controlled by the GaSb layer thickness shown in Fig 1b. When we account for the difference in atomic density between GaN and GaSb, the intended effective percentage of Sb in the active region ranged from 0 up to 61% Sb, as shown in Fig 1c. Note that samples 4 and 5 have the same intended overall Sb composition and similar overall thickness, but with considerable differences in the layer thicknesses and number of periods.

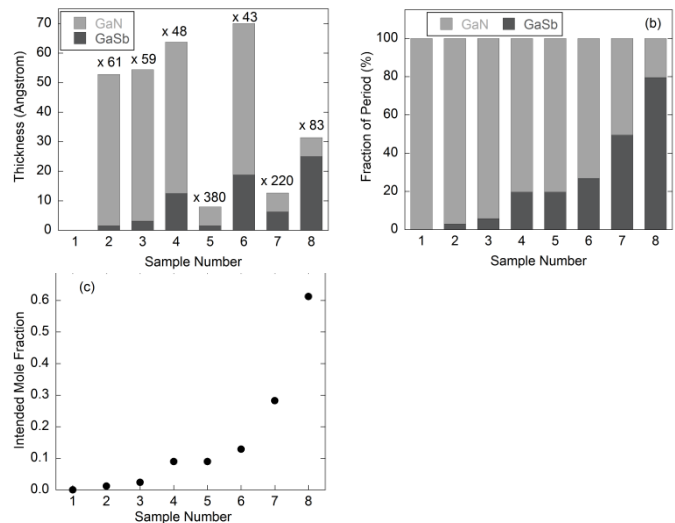


Fig. 1. Thicknesses of the GaN and GaSb layers in the periodic structures and intended Sb mole fraction. (a) The various repeating cell thicknesses and number of periods, (b) the relative percentage of the structure controlled by the GaSb layer thickness, (c) the expected effective percentage of Sb in the active region.

3. RESULTS AND DISCUSSION

Figure 2 summarizes the compositions of the films as measured by RBS and WDS. Since the wafer was quartered and different pieces were sent to separate labs for RBS and WDS, the exact same area was not

measured, although in both cases measurements were taken near the center of the 2-inch wafer (corresponding to the 90 degree corner of the quartered wafer). The WDS and RBS measurements agree within a mole fraction of +/- 0.01 with the exception of samples 7 and 8. The discrepancy comes from the differences in depth sensitivity of the two methods: WDS gives a single number averaged over an excitation volume 100s of nm deep, while RBS is a depth profiling technique. Samples 7 and 8 are very thin and the cap and buffers layers make up a larger fraction of the region sampled by the WDS. The RBS results are thus more reliable, with the reported results being the average RBS composition of the entire film. Note that for samples with larger Sb content ($x > 0.2$) the actual composition is lower than the intended design composition. Although we close the N shutter during the GaSb layer growths, we cannot completely shut off the N flux since it leaks around the shutter throughout the growth. Therefore, growing pure GaSb layers with current technology is likely not possible, and the samples designed to consist of more GaSb will have a larger discrepancy between the intended and measured concentration in Sb. Furthermore, as reported for the intentionally grown bulk alloys, the amount of Sb that incorporates into the film saturates at a value dependent on temperature and growth rate, even in the presence of additional Sb relative to N.

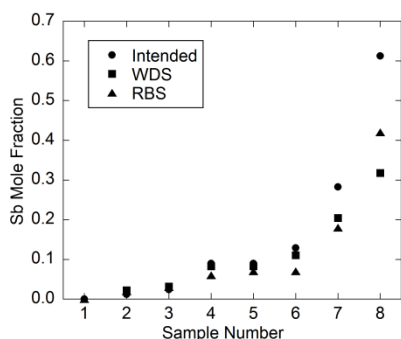


Fig. 2. Measured and intended concentrations of Sb in the films

The bandgaps of the samples were determined from optical absorption measurements. As shown in Figure 3 the bandgaps decrease with the Sb composition (measured by RBS) as predicted by a modified band anticrossing (BAC) model that is applicable to HMAs in the entire composition range [26]. The BAC model describes the perturbation of the GaN valence band by the localized Sb level. The localized Sb level is estimated to lie 1.2 eV above the GaN valence band edge, and the interaction between this level and that of the GaN valence band causes the valence band to split into two sub-bands, the E+ and the E- band. The anticrossing-interaction leads to the E+ level lying above the Sb level and the E- level below the level. This means that introducing Sb to GaN immediately leads to a large upwards shift of GaNSb valence band by at least 1.2 eV. Adding additional Sb to the ternary alloy will push the E+ band further upwards leading to an even smaller band gap; however, it will not have as drastic of an effect as the initial introduction of Sb into GaN. We note that this is an effect of the anticrossing interaction described by the BAC model and not a new feature of the modified model.

Samples with the same overall effective Sb composition have similar bandgap as those previously measured and reported for thin film $\text{GaN}_{1-x}\text{Sb}_x$ alloys grown with no shutter cycling [21-23]. This seems to suggest that both methods produce homogeneous bulk alloys.

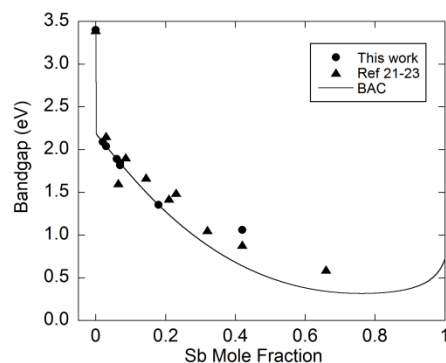


Fig. 3. Measured bandgap as a function of Sb concentration (RBS) and fit according to the modified BAC.

The designed structure of both samples 4 and 5 have very different layer thicknesses and number of periods but had the same overall average target composition. The RBS/WDS and optical absorption measurements show similar results within the experimental errors for the two samples. The compositions of samples 4 and 5 were 6% and 7% as measured by RBS. The composition as measured by WDS was 7% for both samples. The bandgaps were 1.89 and 1.84 eV, respectively. These results suggest that resulting alloy's composition is dependent only on the proportion of GaSb designed into the structure, achieved with different thicknesses of GaSb and GaN layers with a correspondingly different number of Sb cycling periods.

We examined selected samples with TEM, and found a range of crystal morphologies. Fig 4(a) and (b) shows the sample grown with no Sb. The structure is columnar, as typical for GaN grown with no accommodations made for the large lattice mismatch with the sapphire substrate. The average column width, measured halfway between the interface with the substrate and the film surface, is 11 nm. The columns get slightly wider throughout the thickness towards the surface. The polycrystalline grains primarily consist of 2H GaN with the (0002) plane oriented in line with the (0006) sapphire substrate planes, but the grains are randomly oriented in-plane. The rough (~10.3 nm average roughness), faceted surface (Fig 4b) is consistent with non-amorphous, polycrystalline GaN grown with no strain remediation.

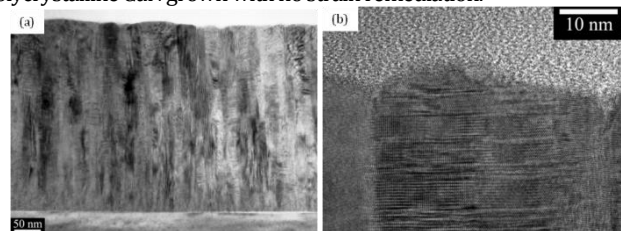


Fig. 4. TEM cross section of sample 1 with no Sb. (a) The entire structure and (b) the faceted surface.

The morphology changes even with small incorporations of Sb. Sample 2 (not shown here), with 2% Sb, had slightly wider columns (15 nm). The surface roughness decreased by 26% relative to the sample with no Sb. The grains were still primarily 2H, but they appear slightly misoriented with respect to the growth direction. We see no evidence of Sb clustering and the interfaces between the active region and both the cap and buffer layer are not visible. There are no horizontal features indicating alternating GaN and GaSb layers.

A high resolution cross sectional image of the GaN buffer layer/GaN-GaSb active region of sample 4 (6% Sb by RBS) is shown in Fig 5. The arrow denotes the interface. The GaN has the typical 2H appearance.

The active region consists of non-columnar, randomly oriented grains with no evidence of either Sb clusters or a multilayer structure.

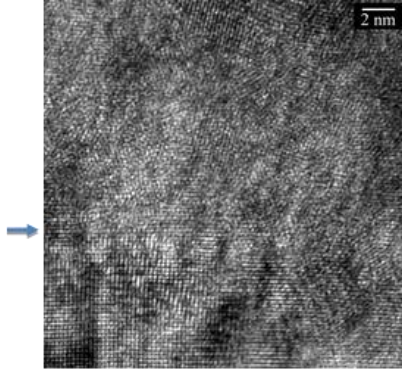


Fig. 5. TEM cross section of sample 4 with targeted GaSb/GaN thicknesses of 12.5 Å/51.3 Å and a measured RBS Sb mole fraction of 6%.

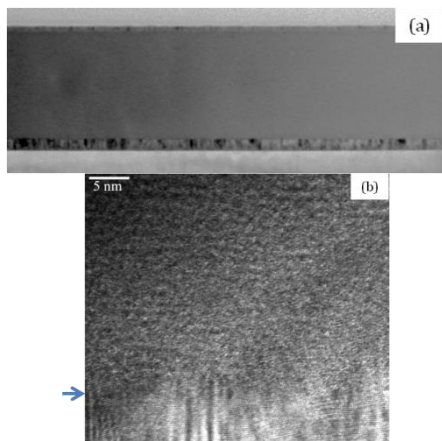


Fig. 6. TEM cross-section of sample 7 with targeted GaSb/GaN thicknesses of 6.25 Å/6.41 Å and an RBS measured concentration of 18% Sb. (a) is a low resolution image showing the entire thickness of the structure, including the sapphire substrate, GaN buffer layer, GaSb/GaN region, and the GaN cap layer. (b) is a higher resolution image showing the top of the GaN buffer layer and the bottom of the GaSb/GaN region, with weak periodic contrast oscillations along the growth direction.

Sample 7 (18% Sb) is shown in figure 6a. Note the abruptness of the interfaces between both the cap and the buffer layer and the active region. This indicates the confinement of Sb to the active region, which has a flat, abrupt interface with the cap layer. The active region consists of very small polycrystalline-amorphous grains, as shown in Fig 6b. This is the only sample that has any evidence of a periodic structure, as lateral, wavy lines of contrast. However, as with all of the other structures in this study, the XRD showed no evidence of a periodic structure. Despite the appearance of segregation, the BAC model still provides a good description of the electronic band structure of the sample [26].

Sample 8 (42% Sb) shows some evidence of Sb clustering, but no evidence of periodic structures. The material is a poly-amorphous mix. The top interface between the active region and the cap is jagged. This is the only sample that did not agree with the BAC model, as it had a bandgap of about 1 eV rather than the predicted 0.7 eV. A significant fraction of Sb forms clusters reducing the concentration of the substitutional Sb that contributes to the band gap reduction in the BAC model.

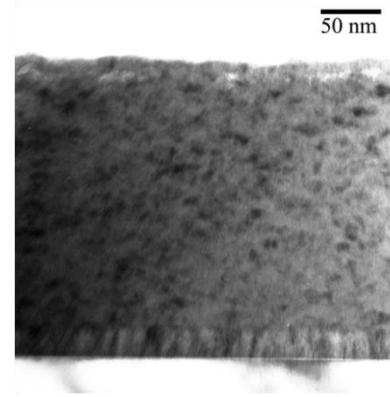


Fig. 7. TEM image of sample 8 with targeted GaSb/GaN thicknesses of 25 Å/6.41 Å and a measured Sb mole fraction of 42%.

We examined all of the structures with XRD, and none of the spectra showed any evidence of satellite peaks or any other feature that indicates a periodic structure. The XRD spectra are indistinguishable from that of bulk alloys having similar compositions.

4. CONCLUSION

Prior experiments with $\text{GaN}_{1-x}\text{As}_x$ and the tendency of Sb to surface indicated that $\text{GaN}_{1-x}\text{Sb}_x$ would likely suffer from phase segregation, particularly at low growth temperatures. Theoretical predictions indicate that $\text{GaN}_{1-x}\text{Sb}_x$ alloys with ~5-7% Sb are a suitable semiconductor candidate for PEC applications. To develop this alloy, we needed to determine the extent of phase segregation, if any, for films grown with low substrate temperatures that allowed Sb incorporation. This experiment induced conditions that would have greatly favored segregation by cycling the Sb shutter during growth.

We find that Sb does not segregate for overall compositions of less than 18% and that interdiffusion dominates. We are interested in Sb compositions below 10%, and for those compositions, growing the structures with Sb and N cycling seems to create a bulk $\text{GaN}_{1-x}\text{As}_x$ alloy. Furthermore, the film maintained a high level of crystallinity (although a polycrystal) for Sb compositions above which had been achieved in intentionally grown bulk layers with no Sb layers. The columnar nature of the films diminished much earlier for the samples grown with Sb cycling (at 6% Sb rather than the 10% Sb seen in the bulk alloys). Since the Sb composition decreases with increasing growth temperatures, we can grow some of the higher Sb containing designs (samples 7-8) at higher temperatures with the intention of producing a higher Sb containing film with improved crystallinity. It is possible that higher temperatures could produce a multilayer structure, since higher temperatures enhances segregation.

Funding. EPSRC (EP/I004203/1); US Army Research Office and ITC-Atlantic (W911NF-12-2-0003); U.S. Department of Energy, Office of Science, Basic Energy Sciences, Materials Sciences and Engineering Division (DE-AC02-05CH11231); General Research Fund of the Research Grants Council of Hong Kong SAR, China (# 11303715). There are no EPSRC-related datasets associated with this publication.

Acknowledgment. MBE growth and TEM were performed at the Army Research Laboratory. RBS and optical measurements and the data analysis performed at Lawrence Berkeley National Laboratories. WDS was performed at the University of Strathclyde.

References

1. T. Flack, B. Pushpakaran, S. Bayne, "GaN technology for power electronic applications: a review." *J. Electron. Mater.* **45**, 2673 (2016).
2. B. J. Baliga, "Gallium nitride devices for power electronic applications," *Semiconductor Science and Technology*, **28**, 074011 (2013)
3. S. Nikishin, B. Borisov, V. Kuryatkov, M. Holtz, G.A. Gartett, W.L. Sarney, A.V. Sampath, H. Shen, M. Wraback, A. Usikov, V. Dmitriev, "Deep UV light emitting diodes grown by gas source molecular beam epitaxy," *J. Materials Science:Materials in Electronics*, **19**, 764 (2008).
4. C.J. Collins, A.V. Sampath, G.A. Garrett, W.L. Sarney, H. Shen, M. Wraback, A. Nikiforov, G.S. Cargill, V. Dierolf, "Enhanced room-temperature luminescence efficiency through carrier localization in AlGaIn alloys, *Appl. Phys. Lett.* **86**, 031916 (2005).
5. A.V. Sampath, G.A. Garrett, C.J. Collins, W.L. Sarney, E.A. Readinger, P.G. Newman, H. Shen, M. Wraback, "Growth of AlGaIn alloys exhibiting enhanced luminescence efficiency," *J Electron Mat.* **35**, 641 (2006).
6. D. Wang, S.P. Svensson, L. Shterengas, G. Belenky, C.S. Kim, I. Vurgaftman, J.R. Meyer, "Band edge optical transitions in dilute-nitride GaNSb," *J. Appl. Phys.* **105**, 014904 (2009).
7. D. Wang, S.P. Svensson, L. Shterengas, G. Belenky, Near band edge optical absorption and photoluminescence dynamics in bulk InAsN dilute-nitride materials, *J. Cryst. Growth*, **312**, 2705 (2010).
8. W.L. Sarney, and S.P. Svensson, Discrepancies in the nature of nitrogen incorporation in dilute-nitride GaSbN and GaAsN films, *J. Vac. Sci. Technol. B* **31** (5), 051206 (2013).
9. W.L. Sarney, S.P. Svensson, S.V. Novikov, K.M. Yu, W. Walukiewicz, M. Ting, C.T. Foxon, "Exploration of the growth parameter space for MBE-grown GaNSb highly mismatched alloys," *J Crystal Growth* **425**, 255 (2015).
10. S.V. Novikov, M. Ting, K.M. Yu, W.L. Sarney, R.W. Martin, S.P. Svensson, W. Walukiewicz, C.T. Foxon, "Tellurium n-type doping of highly mismatched amorphous GaNAs alloys in by plasma-assisted molecular beam epitaxy," *J Cryst. Growth* **404**, 9 (2014).
11. W. Shan, W. Walukiewicz, K.M. Yu, J.W. Ager, E.E. Haller, J.F. Geisz, D.J. Friedman, J.M. Olson, Sarah Kurtz, C. Nauka, "Effect of nitrogen on the electronic band structure of group III-N-V alloys," *Phys. Rev. B.* **62**, 4211 (2000).
12. R. M. Sheetz, E. Richter, A. N. Andriotis, S. Lisenkov, S. Pendyala, M. K. Sunkara, and M. Menon, "Visible light absorption and large band gap bowing in dilute alloys of gallium nitride with antimony," *Phys. Rev. B.* **84**, 075304 (2011).
13. S.V. Novikov, A.J. Wisner, A. Bell, I. Harrison, T. Li, R.P. Campion, C.R. Staddon, C.S. Davis, F.A. Ponce, C.T. Foxon, "The transition from As-doped GaN, showing blue emission, to GaNAs alloys in films grown by molecular beam epitaxy," *J. Crystal Growth* **240**, 423 (2002).
14. R. Kuroiwa, H. Asahi, K. Asami, S.-J. Kim, K. Iwata, and S. Gonda, "Optical properties of GaN-rich side of GaNP and GaNAs alloys grown by gas-source molecular beam epitaxy," *Appl Phys Lett*, **73**, 2630 (1998).
15. K. Iwata, H. Asahi, K. Asami, R. Kuroiwa, S. Gonda, "GaN-rich side of GaNAs grown by molecular beam epitaxy," *Jpn. J. Appl. Phys.* **37**, 1436 (1998).
16. Y. Zhao, F. Deng, S. S. Lau, and C. W. Tu, "Effects of arsenic in gas-source molecular beam epitaxy," *J Vac Sci B* **16**, 1297 (1998).
17. L. Zhang, H.F. Tang, J. Schieke, M. Mavrikakis, and T. F. Kuech, "The addition of Sb as a surfactant to GaN growth by metal organozinc vapor phase epitaxy," *J. Appl. Phys.*, **92**, 2304, (2002).
18. K. M. Yu, S. V. Novikov, R. Broesler, I. N. Demchenko, J. D. Denlinger, Z. Liliental-Weber, F. Luckert, R.W. Martin, W. Walukiewicz, C.T. Foxon, "Highly mismatched crystalline and amorphous GaNAs alloys in the whole composition range," *J. Appl. Phys.* **106**, 103709 (2009).
19. M. Copel, M.C. Reuter, M. Horn von Hoegen, and R.M. Tromp, "Influence of surfactants in Ge and Si epitaxy on Si (001)." *Phys Rev B* **42**, 682 (1990).
20. M. Copel, M.C Reuter, Efthimios Kaxiras, and R.M. Tromp, "Surfactants in epitaxial growth," *Phys. Rev. B* **63**, 632 (1989).
21. K.M. Yu, W.L. Sarney, S.V. Novikov, D. Detert, R. Zhao, J.D. Denlinger, S.P. Svensson, O.D. Dubon, W. Walukiewicz, C.T. Foxon, "Highly mismatched N-rich GaNSb films grown by low temperature molecular beam epitaxy," *Appl. Phys. Lett.* **102**, 102104 (2013).
22. K. M. Yu, S. V. Novikov, Min Ting, W. L. Sarney, S.P. Svensson, M. Shaw, R. W. Martin, W. Walukiewicz, and C. T. Foxon, "Growth and characterization of highly mismatched GaN_{1-x}Sb_x," *J. Appl. Phys.* **116**, 123704 (2014).
23. W.L. Sarney, S.P. Svensson, S.V. Novikov, K.M. Yu, W. Walukiewicz, C.T. Foxon, "GaNSb highly mismatched alloys grown by low temperature molecular beam epitaxy under Ga-rich conditions," *J. Cryst. Growth* **383**, 9 (2013).
24. W.L. Sarney, S.P. Svensson, "Discrepancies in the nature of nitrogen incorporation in dilute-nitride GaSbN and GaAsN films," *J. Vac. Sci. B*, **31**, 51206 (2013).
25. H. Nair, A. Crook, K.M. Yu, S.R. Bank, "Structural and optical studies of nitrogen incorporation into GaSb-based GaInSb quantum wells," *Appl. Phys. Lett.* **100**, 021103 (2012).
26. N. Segercrantz, K. M. Yu, M. Ting, W. L. Sarney, S.P. Svensson, S. V. Novikov, C. T. Foxon and W. Walukiewicz, "Electronic band structure of highly mismatched GaN_{1-x}Sb_x alloys in a broad composition range," *Appl. Phys. Lett.* **107**, 142104 (2015).